

RESEARCH

Open Access



# Digestion characteristics of sweet potato (*Ipomoea batatas*) polysaccharide in vitro and its relieving effect on ability to relieve exercise fatigue in mice

Xiao Gong<sup>1\*</sup>, Wei-ze Mao<sup>1</sup>, Tian Xu<sup>2</sup>, Le Luo<sup>1</sup> and Xiao-jing Chen<sup>1</sup>

## Abstract

The characteristics of *Ipomoea batatas* polysaccharide (IBP) in vitro and its anti-fatigue effects on exercise fatigue in mice were investigated. The dynamic division of IBP was simulated in vitro, and the structural changes in IBP were analyzed by Fourier Transform Infra-Red (FTIR) and High Performance Liquid Chromatography (HPLC). The results revealed that no free monosaccharides were produced after simulated division in vitro. The CH<sub>2</sub> signal gradually disappeared in the gastric juices after digestion, and the peak attributed to COO asymmetric vibration shifted to the longwave strength in the gastrointestinal juices after digestion. The mean exhaustive swimming time of each IBP dose group was significantly different from that of the blank control group ( $P < 0.05$ ); in particular, the exhaustive swimming time of the high-dose group increased by 81%, the contents of muscle glycogen and liver glycogen were significantly greater than those of the blank control group ( $P < 0.05$ ), the MDA equivalents for Thiobarbituric Acid Reactive Substances (TBARS) of exhaustive swimming mice in each IBP dose group decreased significantly ( $P < 0.05$ ), and the activities of SOD, CAT, and GPx in the high-dose group increased by 61%, 89%, and 72%, respectively, compared with those in the blank control group. IBP could effectively relieve exercise fatigue and provide new raw materials for use as dietary supplements.

**Keywords** *Ipomoea batatas* polysaccharide, *In vitro* digitization, Anti-fatigue, Serum, Swimming mice

## Graphical Abstract

Note: Gastrodigestive products were from *Ipomoea batatas* polysaccharide after dynamic simulated gastric digestion *in vitro*; gastrointestinal digestive products were from *Ipomoea batatas* polysaccharide after dynamic simulated gastrointestinal digestion *in vitro*. Blank Control group (BC), Taurine Control group (TC), Low dose *Ipomoea Batatas* Polysaccharide (IBPL), middle dose *Ipomoea Batatas* Polysaccharide (IBPM) and high dose *Ipomoea Batatas* Polysaccharide (IBPH).

\*Correspondence:

Xiao Gong

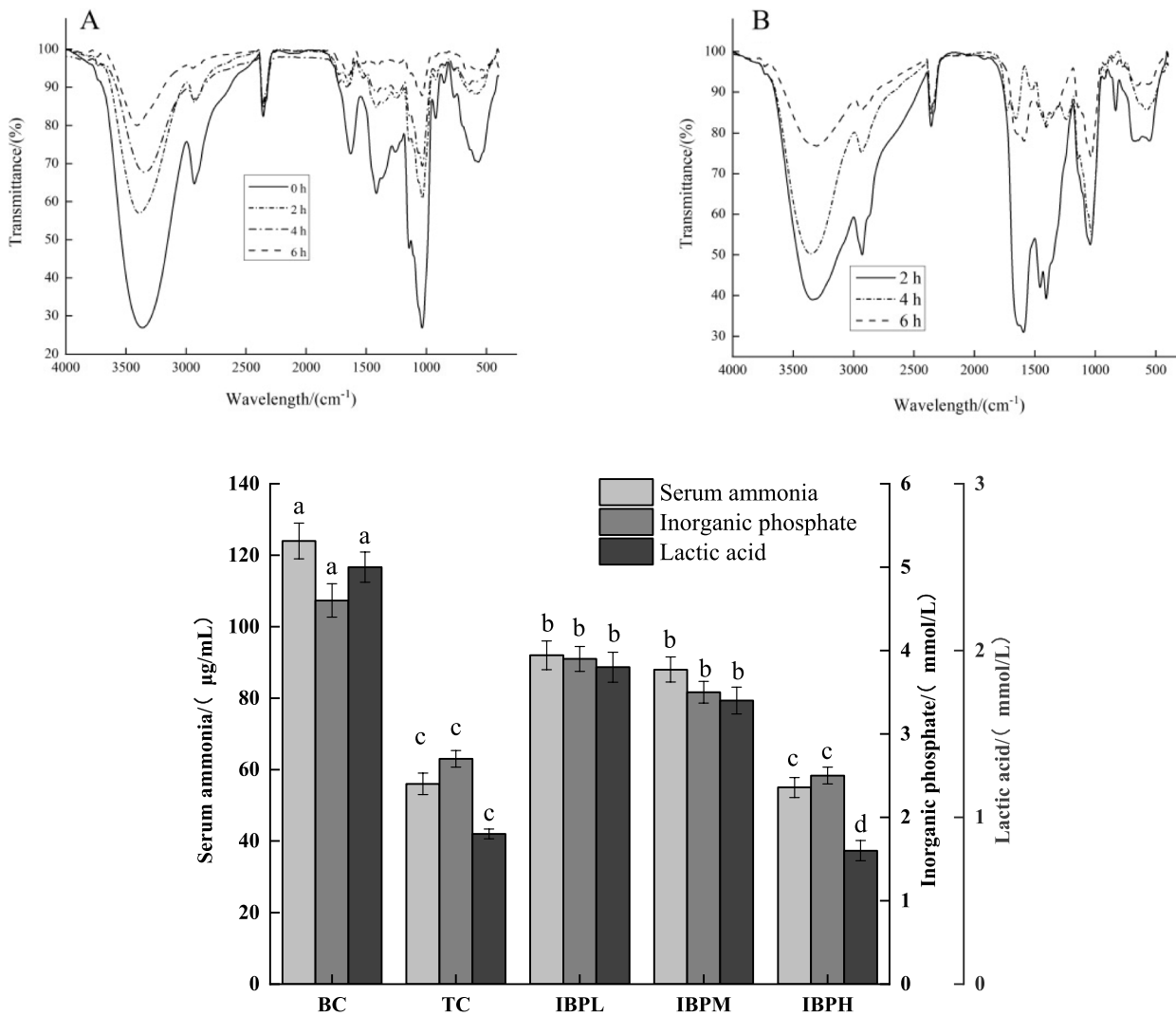
[gongxiao0221@126.com](mailto:gongxiao0221@126.com)

Full list of author information is available at the end of the article



© The Author(s) 2025. **Open Access** This article is licensed under a Creative Commons Attribution 4.0 International License, which permits use, sharing, adaptation, distribution and reproduction in any medium or format, as long as you give appropriate credit to the original author(s) and the source, provide a link to the Creative Commons licence, and indicate if changes were made. The images or other third party material in this article are included in the article's Creative Commons licence, unless indicated otherwise in a credit line to the material. If material is not included in the article's Creative Commons licence and your intended use is not permitted by statutory regulation or exceeds the permitted use, you will need to obtain permission directly from the copyright holder. To view a copy of this licence, visit <http://creativecommons.org/licenses/by/4.0/>.

Analysis of the digestive infraredspectra of gastric juice (A), gastrointestinal juice (B) and effects of *Ipomoea batatas* polysaccharide on the levels of serum ammonia, inorganic phosphate, and lactic acid in exhaustive swimming mice



### Introduction

Sweet potato (*Ipomoea batatas*) is classified as a convulvaceae and is an annual dicotyledonous herb that is rich in protein, polyphenols, vitamins, minerals, and other active compounds (Tang et al., 2018; Iwuoha et al., 2022). In particular, researchers have paid increasing attention to *Ipomoea batatas* polysaccharide (Huang et al., 2021). The polysaccharide extract of *Ipomoea batatas* has many biological activities, such as antioxidant, hypoglycemic, liver protection, anticancer, and regulatory effects on the intestinal flora (Yang et al., 2021; Zhao et al., 2005; Tian et al., 2008). Plant polysaccharides, such

as maca polysaccharides (Lee et al., 2020), Schisandra chinensis polysaccharides (Shan et al., 2019), Tricholoma matsutake polysaccharides (An et al., 2023), and turnip polysaccharides (Zhao et al., 2021), have strong anti-fatigue effects. Plant polysaccharides enhance the exercise ability of mice by improving free radical metabolism and glucose metabolism, resulting in strong anti-fatigue effects. However, there are few related reports on the antifatigue activity of polysaccharides from *Ipomoea batatas*.

Exercise fatigue is a complex physiological phenomenon caused by mental or physical exhaustion. The

main factors that cause fatigue include decreases in the blood sugar level and tissue glycogen content and excessive production and accumulation of metabolites, such as lactate and nitrogen in the urine (Bellenger et al., 2016; Mehta et al., 2012). Although many factors cause fatigue, oxidative stress is considered to play a key role. After excessive exercise, the liver, muscles and other organs produce excessive reactive oxygen species, which can cause cell metabolism disorders and lipid peroxidation and damage skeletal muscle and liver mitochondria, thus causing fatigue (Qu et al., 2022; Gilstrap et al., 2021). At present, a common method to relieve fatigue is to take drugs or nutritional supplements, but taking drugs has many side effects, such as calcium loss, abnormal blood sugar and blood lipid metabolism, cardiovascular diseases, and impaired liver function (Zhang et al., 2021). The primary chemical properties and anti-fatigue effects of the *Pholiota nameko* polysaccharide (PNP) were explored, and PNP was shown to have an anti-fatigue effect in vivo (Zhang et al., 2021). Therefore, natural polysaccharides can be used as nutritional supplements to regulate exercise fatigue.

The digestion characteristics of *Ipomoea batatas* polysaccharide were determined in vitro, and specific pathogen-free (SPF) mice were used as the research object. The ability of the *Ipomoea batatas* polysaccharide to relieve exercise fatigue in mice was determined systematically, and the changes in physiological and biochemical indices related to fatigue were evaluated to provide a scientific basis for exploring the alleviation of exercise fatigue and the comprehensive use of the *Ipomoea batatas* polysaccharide.

## Materials and methods

### Materials and reagents

*Ipomoea batatas* plants were purchased from local supermarkets

Gastric juice simulation solution, intestinal juice simulation solution (Suzhou Xiaodong Yijian Instrument and Equipment Co., Ltd.); specific pathogen-free (SPF) male mice (20–25 g/mouse, Nanjing Institute of Biomedicine); a malondialdehyde (MDA) enzyme-linked immunosorbent assay (ELISA) kit, a liver/muscle glycogen detection kit, a lactic acid detection kit (Shanghai Biotechnology Co., Ltd.); inorganic phosphate, serum ammonia, superoxide dismutase (SOD), catalase (CAT), and glutathione peroxidase (GPX) detection kits (Shenzhen Ruiqing Bioinformation Technology Co., Ltd.); taurine, acetic acid, potassium hydroxide, ethanol, ether, and other chemicals (analytical grade, pure) (Tianjin Kemio Reagent Co., Ltd.).

### Instruments and equipment

A DIVRS-II Plus in vitro bionic rat stomach digestive system (Suzhou Xiaodong Yijian Instrument Equipment Co., Ltd.); a TENSOR 27 Fourier Transform Infrared Spectrometer (Beijing Haikē Sirui Optoelectronic Instrument Co., Ltd.); a Waters E2695 High Performance Liquid Chromatograph (Waters Technology (Shanghai) Co., Ltd.); a DB080 mouse constant temperature swimming box (diameter 410 mm, height 400 mm) (Beijing Zhishu Duobao Biotechnology Co., Ltd.); a 5430R refrigeration centrifuge (Eppendorf Company of Germany); a DHG-9240 blast drying oven (Qingdao Dongfei Keyi Environmental Protection Technology Co., Ltd.); a HH-12 A constant-temperature water bath (Changzhou Runhua Electric Appliance Co., Ltd.); a QE-400 high-speed crusher (Zhejiang Yili Industry and Trade Co., Ltd.); a G9800A microplate reader (Thermo Fisher Technology Company, USA).

### Preparation of *Ipomoea batatas* polysaccharide

One kilogram of *Ipomoea batatas* was weighed accurately after cleaning and being smashed into pieces. Two liters of distilled water were added to the sample, which was subsequently filtered to remove starch, and the sample was then cleaned 3 times until the starch was completely removed. The *Ipomoea batatas* residue powder was placed in an oven at 60 °C for 12 h, after which it was removed and crushed for later use. One hundred grams of *Ipomoea batatas* residue powder was extracted with 0.06 mol/L sodium hydroxide solution at a ratio of 1:20 (g/mL) in a water bath at 80 °C for 1.5 h and then centrifuged at 4,700 × g for 10 min to obtain the crude polysaccharide extract of *Ipomoea batatas*. The supernatant was added to 4 volumes of absolute ethanol, incubated at room temperature for 40 min, and centrifuged at 7,500 × g for 10 min to obtain the *Ipomoea batatas* polysaccharide. Then, the crude *Ipomoea batatas* polysaccharide was dissolved in 2 mL of distilled water, placed in a 4000-u dialysis bag, dialyzed at 4 °C for 48 h, and then freeze-dried to obtain the *Ipomoea batatas* polysaccharide (IBP) (Marzi et al., 2022).

### Simulated stomach and gastrointestinal digestion

Five milliliters of IBP (5 mg/mL) and 0.6 mL of gastric juice (fasting gastric juice) were injected into a rat stomach containing bionic silica gel, and then, the gastric juice and intestinal juice were sucked into a special syringe. The silica gel bionic rat stomach, gastric juice, intestinal juice, and silica gel bionic intestinal tract were installed, and the special syringe was emptied. The injection speed of the simulated gastric fluid was 25 µL/min, the injection speed of the simulated intestinal fluid was 30 µL/min, the

chyme emptying speed was 100  $\mu\text{L}/\text{min}$ , the gastric compression frequency was 3 rpm, the pyloric compression frequency was 10 rpm, the gastric rolling frequency was 12 rpm, the intestinal rolling frequency was 36 rpm, the gastric tilt speed was  $0.05^\circ/\text{min}$ , and the running time was 2, 4, or 6 h. After the operation, 3 mL samples were taken from the stomach and intestine of silica gel bionic rats and placed in boiling water for enzyme inactivation (Liu et al., 2022).

#### HPLC analysis

The amount of free monosaccharide produced from the simulated digestion of IBP was determined by PMP pre-column derivatization. The detection conditions included a Sunfire C18 column (4.6 mm  $\times$  150 mm, 5  $\mu\text{m}$ , USA). The mobile phase was a 0.1 M phosphate buffer solution with a pH of 6.7 and acetonitrile with a volume ratio of 83:17; the flow rate was 1 ml/min; the column temperature was 30  $^\circ\text{C}$ ; and the detection wavelength was 245 nm.

#### Fourier transform infrared spectroscopy analysis

The IBP and potassium bromide were mixed at a ratio of 1:50, and a small number of mixed samples were taken, placed in a mortar, evenly ground under a baking lamp, pressed into tablets, and scanned in the range of 400–4,000  $\text{cm}^{-1}$ .

#### Mouse rearing

Sixty male SPF mice weighing 18–20 g were fed at a room temperature ranging from 22 to 24  $^\circ\text{C}$  and a relative humidity ranging from 40 to 50% for one week. The mice were randomly divided into 5 groups with 12 mice in each group: the blank control group (BC), taurine control group (TC), low-dose IBP group (IBPL), middle-dose IBP group (IBPM) or high-dose IBP group (IBPH). The mice were subjected to intragastric administration at 10:00 am every day for 28 days. The blank control group was fed distilled water, and the specific intragastric volume was calculated based on the body weights of the mice in the different IBP groups and the taurine control group. The intragastric doses used for the low, medium, and high IBP groups and the taurine control group were 50, 100, 200 and 200 mg/kg, respectively. The mice were trained to swim once a day for 20 min (Wei et al., 2017).

#### Exhaustive swimming test

After 28 days of feeding, the 4 groups of mice were forced to swim continuously in a cylindrical swimming box with a diameter of 410 mm, a height of 400 mm and a water temperature of 25  $^\circ\text{C}$ . The time when the mice could not surface after exhaustion lasted 9 s, which was recorded

as the exhaustive swimming time of the mice (Wei et al., 2017).

#### Sample collection

After the exhaustive swimming test, blood was drawn from the eyeballs of the mice, and the samples were incubated at room temperature for 30 min. The samples were subsequently centrifuged at 4  $^\circ\text{C}$  and  $2,800 \times g$  for 15 min, after which the supernatants were collected as serum and stored at 18  $^\circ\text{C}$ . The mice were killed by decapitation after blood collection. The liver and leg muscles were quickly removed, washed with normal saline 3 times, and dried with filter paper. All the collected tissues were quickly frozen in liquid nitrogen and stored at  $-80^\circ\text{C}$ .

#### Determination of fatigue-related physiological and biochemical indices

To determine the glycogen contents in the liver and muscle, the collected liver and muscle tissues of the mice were incubated at room temperature for 30 min, 0.2 g of liver or muscle was weighed, 500  $\mu\text{L}$  of 7.5 mol/L KOH solution was added to each sample to make a homogenate, the mixture was allowed to react in a boiling water bath for 30 min, the mixture was cooled to 25  $^\circ\text{C}$ , 1 mL of absolute ethanol was added, the mixture was centrifuged at  $11,200 \times g$  and 4  $^\circ\text{C}$  for 15 min, the precipitate was discarded, 0.5 mL of anthrone solution with a 0.2% mass–volume ratio was added to the supernatant, and the absorbance at 620 nm was measured.

The lactic acid content, inorganic phosphate content, and serum ammonia concentration of the prepared serum were detected according to the kit instructions.

Determination of liver antioxidant indices: Malondialdehyde (MDA), superoxide dismutase (SOD), catalase (CAT), and glutathione peroxidase (GPx) activities (Huang et al., 2023) were determined according to the kit instructions.

#### Data analysis

The experimental data are expressed as the means  $\pm$  standard deviations and were analyzed using SPSS 22.0 software.  $P < 0.05$  indicated a significant difference.

#### Determination of the free monosaccharide content of IBP after simulated digestion *in vitro*

The results of the determination of the free monosaccharide in the digested products of the IBP after dynamic simulated gastric digestion *in vitro* are shown in Fig. 1A. No free monosaccharide was produced in the digested products of the stomach. The results of the determination of the free monosaccharide in the digestive products of the IBP after dynamic simulated gastrointestinal

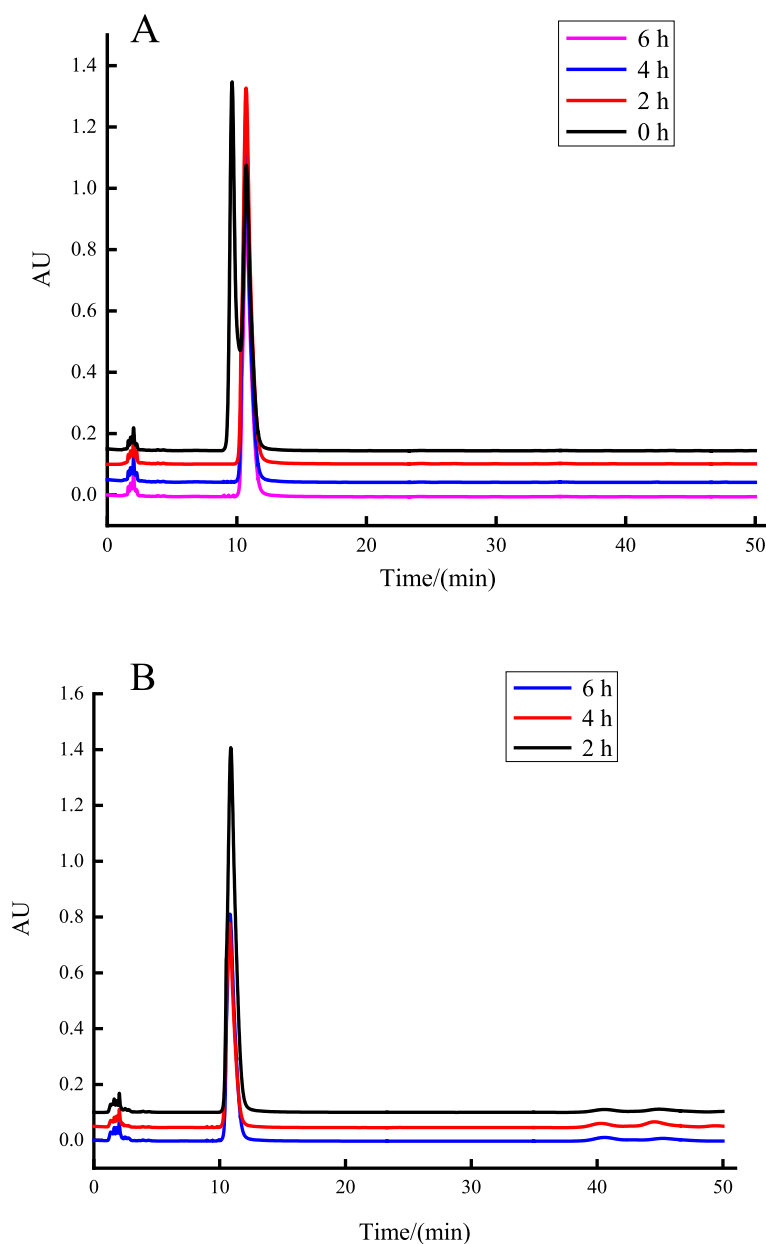


**Fig. 1** HPLC analysis of free monosaccharide from gastrodigestive products (A) and gastrointestinal digestive products (B). Note: Gastrodigestive products were from *Ipomoea batatas* polysaccharide after dynamic simulated gastric digestion *in vitro*; gastrointestinal digestive products were from *Ipomoea batatas* polysaccharide after dynamic simulated gastrointestinal digestion *in vitro*

digestion *in vitro* are shown in Fig. 1B. The formation of free monosaccharide was not detected in the intestinal digestive products, indicating that IBP cannot be digested by gastrointestinal fluid during gastrointestinal digestion.

#### Fourier transform infrared spectroscopy analysis of IBP after simulated digestion

Infrared spectroscopy is an important method for the characterization of substances, and its analysis provides

much information on functional groups, which can help determine some or all molecular types and structures. The results of the infrared spectrum analysis of the IBP digested by the simulated stomach *in vitro* are shown in Fig. 2A. The signals of the digested products at  $3360\text{ cm}^{-1}$ ,  $3371\text{ cm}^{-1}$ ,  $3358\text{ cm}^{-1}$ , and  $3379\text{ cm}^{-1}$  were O-H tensile vibrations, and the absorption peaks of the OH tensile vibrations gradually smoothed from sharp to smooth during 0–6 h of digestion. The signals at  $2931\text{ cm}^{-1}$ ,  $2932$

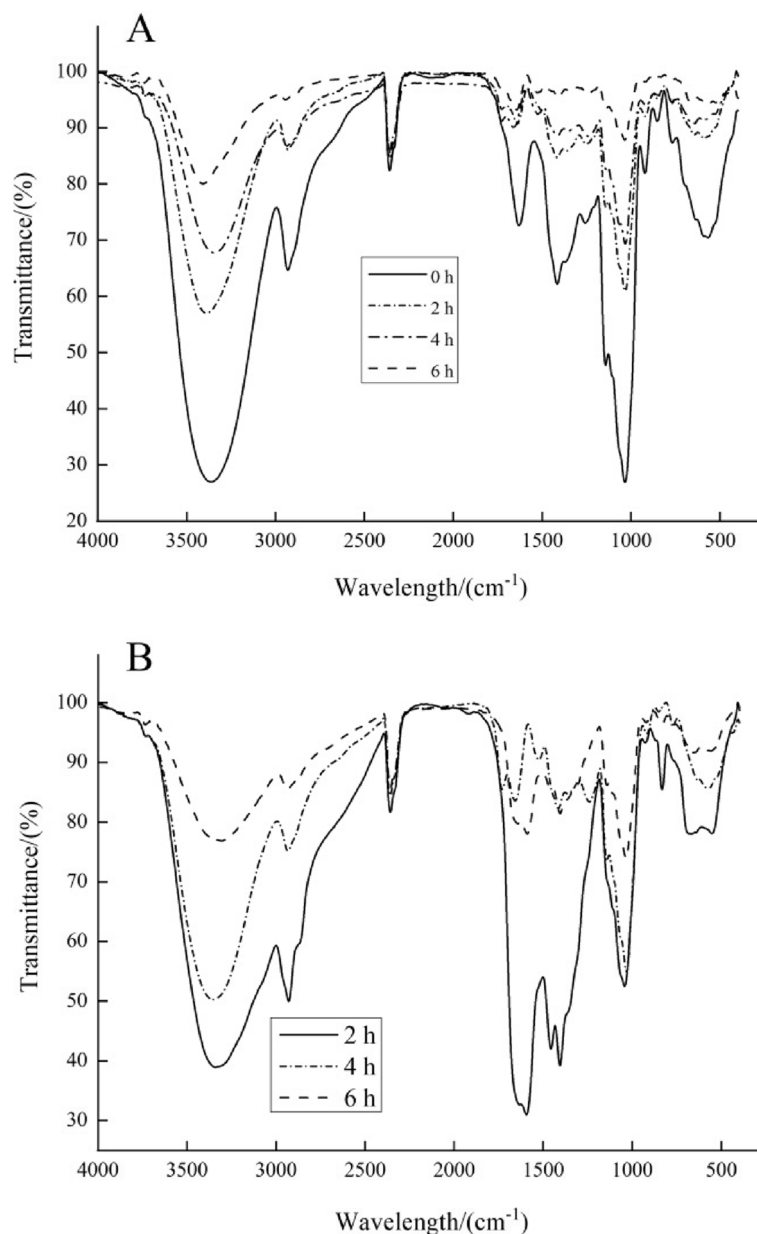


**Fig. 2** Analysis of the digestive infrared spectra of gastric juice (A) and gastrointestinal juice (B)

cm<sup>-1</sup>, 2932 cm<sup>-1</sup> and 2930 cm<sup>-1</sup> were -CH<sub>2</sub> vibration absorption peaks, which almost disappeared after digestion for 6 h. The absorption peak near 2380 cm<sup>-1</sup> was the CO<sub>2</sub> signal, which was caused by CO<sub>2</sub> saturation in the environment. The absorption bands centered at 1631 cm<sup>-1</sup>, 1629 cm<sup>-1</sup>, 1633 cm<sup>-1</sup> and 1630 cm<sup>-1</sup> were caused by the asymmetric stretching bands of COO<sup>-</sup>, which were characteristic absorption peaks of the C=O bond. The signal values at 1415 cm<sup>-1</sup>, 1419 cm<sup>-1</sup>, 1415 cm<sup>-1</sup>, and 1407 cm<sup>-1</sup> were symmetrical stretching vibration peaks of COO<sup>-</sup>, and after 6 h of digestion, the signals also

gradually disappeared. The four digested products all had characteristic absorption peaks of carbohydrates. The results of the infrared spectrum analysis of the digested products of the IBP after simulated gastrointestinal digestion in vitro are shown in Fig. 2B. The signals of the digested products at 3338 cm<sup>-1</sup>, 3345 cm<sup>-1</sup> and 3343 cm<sup>-1</sup> at different digestion times were OH tensile vibrations. The signals at 2929 cm<sup>-1</sup>, 2932 cm<sup>-1</sup> and 2931 cm<sup>-1</sup> were -CH<sub>2</sub> vibration absorption peaks. The absorption peak near 2380 cm<sup>-1</sup> was the CO<sub>2</sub> signal, which was caused by CO<sub>2</sub> saturation in the environment. The absorption bands

centered at  $1595\text{ cm}^{-1}$ ,  $1589\text{ cm}^{-1}$  and  $1633\text{ cm}^{-1}$  were caused by the asymmetric stretching bands of  $\text{COO}^-$ , and the characteristic peaks of the  $\text{COO}^-$  stretching vibration shifted to short wavelengths ( $1589\text{ cm}^{-1}$ ) and then to long wavelengths ( $1633\text{ cm}^{-1}$ ) during digestion for 2–6 h. The signal values at  $1456\text{ cm}^{-1}$ ,  $1459\text{ cm}^{-1}$  and  $1455\text{ cm}^{-1}$  were symmetrical stretching vibration peaks of  $\text{COO}^-$ . The absorption peaks of the three digested products were at  $1250\text{ cm}^{-1}$ ,  $1050\text{ cm}^{-1}$  and  $840\text{ cm}^{-1}$ . These findings are consistent with those of a study by Li (Li et al., 2019) on neutral ginseng polysaccharide.

The results of the infrared spectroscopy of the digestive products revealed that the vibration absorption peaks of O-H and  $-\text{CH}_3$  in the oral digestive products gradually decreased with increasing digestion time after simulated digestion, which may have been caused by changes in the structure. The  $-\text{CH}_2$  signal also gradually disappeared from the digestive products. In the gastrointestinal digestive products, the absorption peak of  $\text{COO}^-$  asymmetric vibration shifted to a greater wave strength, and the absorption peak strength of  $\text{COO}^-$  symmetric tensile vibration decreased significantly. The above structural changes were inferred to be due to the increase in the reducing sugar content.

#### Effect of IBP on exhaustive swimming time in mice

The body's physical fitness and muscle strength decrease with increasing exercise intensity. The most intuitive method to improve anti-fatigue ability is to increase exercise endurance, and the level of exercise endurance

in mice can be intuitively reflected through exhaustive swimming time (Chen et al., 2021). The results are shown in Fig. 3. The average exhaustive swimming time of each IBP dose group was significantly different from that of the blank control group ( $P < 0.05$ ), especially the exhaustive swimming time of the high-dose group, which increased by 81% compared with that of the blank control group, indicating that each IBP dose significantly improved the endurance of exercise in the mice. There were no significant differences between the low- and middle-dose groups ( $P > 0.05$ ), indicating that there was no dose dependence of IBP in the range of 50–100 mg/kg, and there were no significant differences in exhaustive swimming time between the high-dose group and the taurine control group ( $P < 0.05$ ), indicating that the anti-fatigue effect of the high-dose group was equivalent to that of taurine. The results showed that IBP in the range of 50–200 mg/kg could significantly increase the exhaustive swimming time of the mice.

#### Effects of IBP on muscle and liver glycogen reserves in exhaustive swimming mice

Carbohydrates are the main substances involved in body function. The amount of blood sugar in the body gradually decreases when the body exercises at high intensity, and this type of behavior leads to fatigue. Glycogen is an important energy reserve in the body. The blood sugar concentration in the body is maintained by the decomposition of muscle and liver glycogen stores during high-intensity exercise; therefore, the higher its content is, the

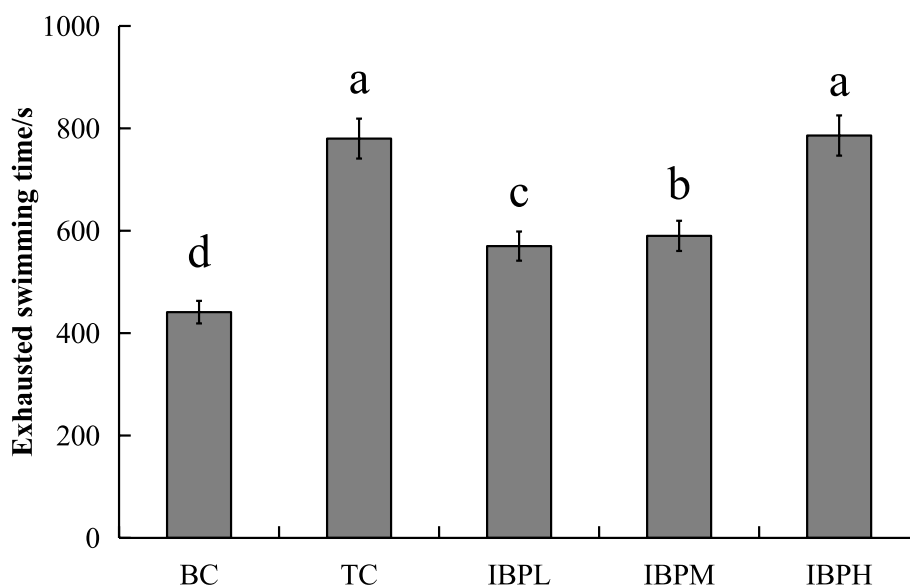


**Fig. 3** Effect of *Ipomoea batatas* polysaccharide (IBP) on exhaustive swimming time in mice ( $n=12$ ). Note: Blank control group (BC), taurine control group (TC), low-dose *Ipomoea batatas* polysaccharide group (IBPL), middle-dose *Ipomoea batatas* polysaccharide group (IBPM) and high-dose *Ipomoea batatas* polysaccharide group (IBPH). Different letters indicate significant differences ( $P < 0.05$ ), the same applies below

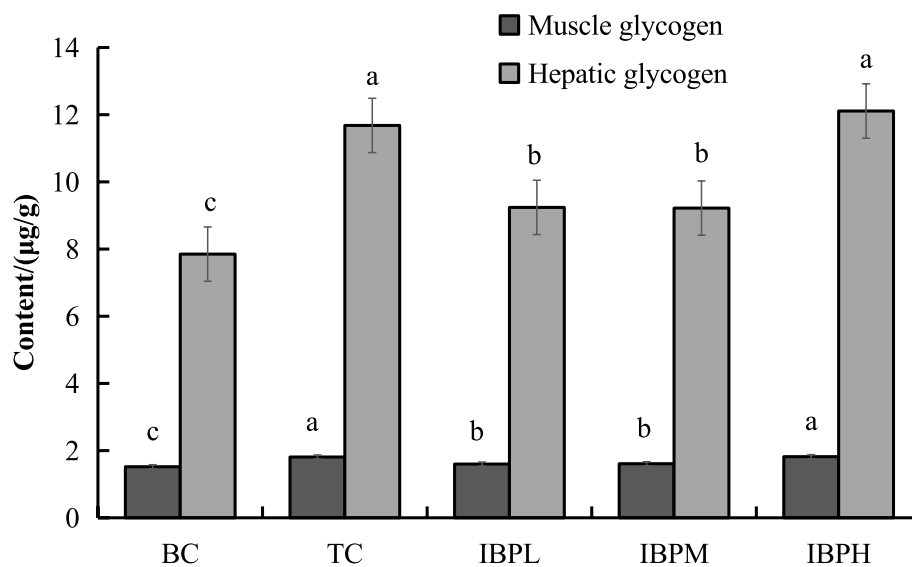


**Fig. 4** Effect of *Ipomoea batatas* polysaccharide (IBP) on glycogen accumulation in the muscle and liver tissues of exhaustive swimming mice ( $n=12$ )

greater the exercise endurance of the body (Liang et al., 2021; Erika & Pablo, 2018). Figure 4 shows the effects of different doses on muscle and liver glycogen stores in exhausted swimming mice. The muscle and liver glycogen contents in the different dose groups were significantly greater than those in the blank control group ( $P < 0.05$ ); in particular, the liver glycogen content in the high-dose group was 58% greater than that in the blank control group and was close to that in the taurine control group. The results showed that IBP in the range of 50–200 mg/kg could significantly increase glycogen synthesis in the muscle and liver tissues of mice, effectively improve exercise endurance, and thus play an anti-fatigue role.

#### Effects of IBP on the levels of serum ammonia, inorganic phosphate, and lactic acid in exhaustive swimming mice

Serum ammonia is produced by protein decomposition during high-intensity exercise, and the more it accumulates in the body, the more severe the fatigue is. The existence of inorganic phosphate in cells acts directly on the transverse bridge of muscle and reduces the sensitivity of muscle fibers, which leads to a decrease in muscle strength. The body produces a large amount of lactic acid, reduces the pH value of blood, changes the steady state of the body during high-intensity exercise, and thus reduces the ability to exercise, which is considered an important factor leading to exercise fatigue (Lee et al., 2015). As shown in Fig. 5, the contents of serum ammonia, inorganic phosphate, and lactic acid in each IBP dose group were significantly lower than those in the blank control

group ( $P < 0.05$ ), especially the lactic acid content in the high-dose group, which was 72% lower than that in the blank control group and significantly lower than that in the taurine control group ( $P < 0.05$ ), consistent with the results reported in the literature (Zhao et al., 2017). The results indicated that IBP in the range of 50–200 mg/kg could reduce the serum ammonia, inorganic phosphate, and lactic acid levels and improve the anti-fatigue capacity of mice.

#### Effects of IBP on liver antioxidant indices in exhaustive swimming mice

Mice produce many free radicals, and the antioxidant system of the body can be destroyed during exhaustive swimming. Therefore, the antioxidant effects of IBP on antioxidant damage and aging were evaluated by measuring the liver antioxidant indices (MDA, SOD, CAT, and GPx) of exhaustive swimming mice (Osman et al., 2018). As shown in Fig. 6, the MDA equivalents for TBARS of exhaustive swimming mice in each IBP dose group were significantly lower ( $P < 0.05$ ) than that in the blank control group, and the higher the IBP content was, the lower the MDA equivalents for TBARS was. The MDA equivalents for TBARS in the high-dose group were equivalent to that in the taurine control group. The activities of SOD, CAT, and GPx increased significantly with increasing IBP content ( $P < 0.05$ ). Compared with those in the control group, the activities of SOD, CAT, and GPx in the high-dose group increased by 61%, 89%, and 72%, respectively. The SOD, CAT, and GPx activities in exhausted mice were positively correlated with the dose of IBP, and the SOD, CAT, and

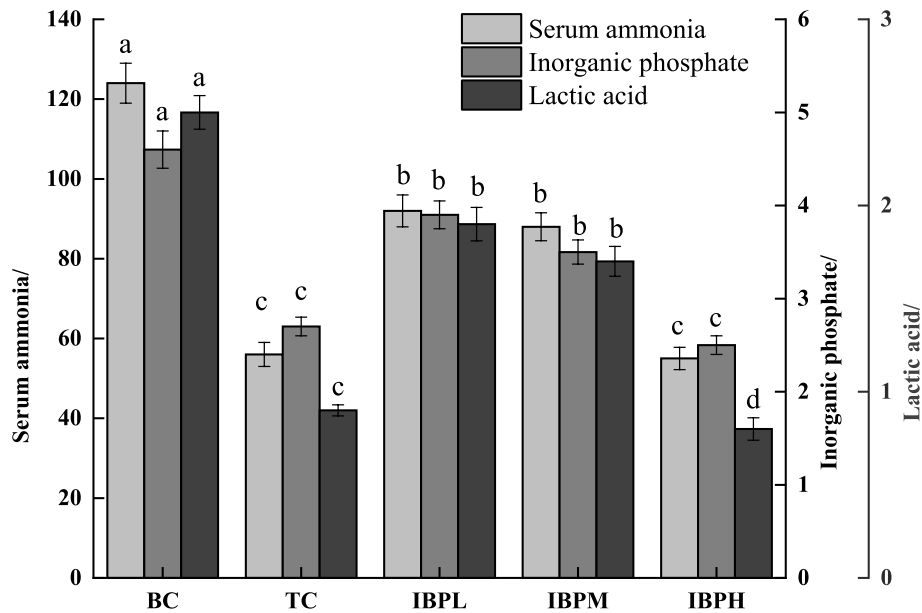


**Fig. 5** Effects of *Ipomoea batatas* polysaccharide (IBP) on the levels of serum ammonia, inorganic phosphate, and lactic acid in exhaustive swimming mice (n=12)

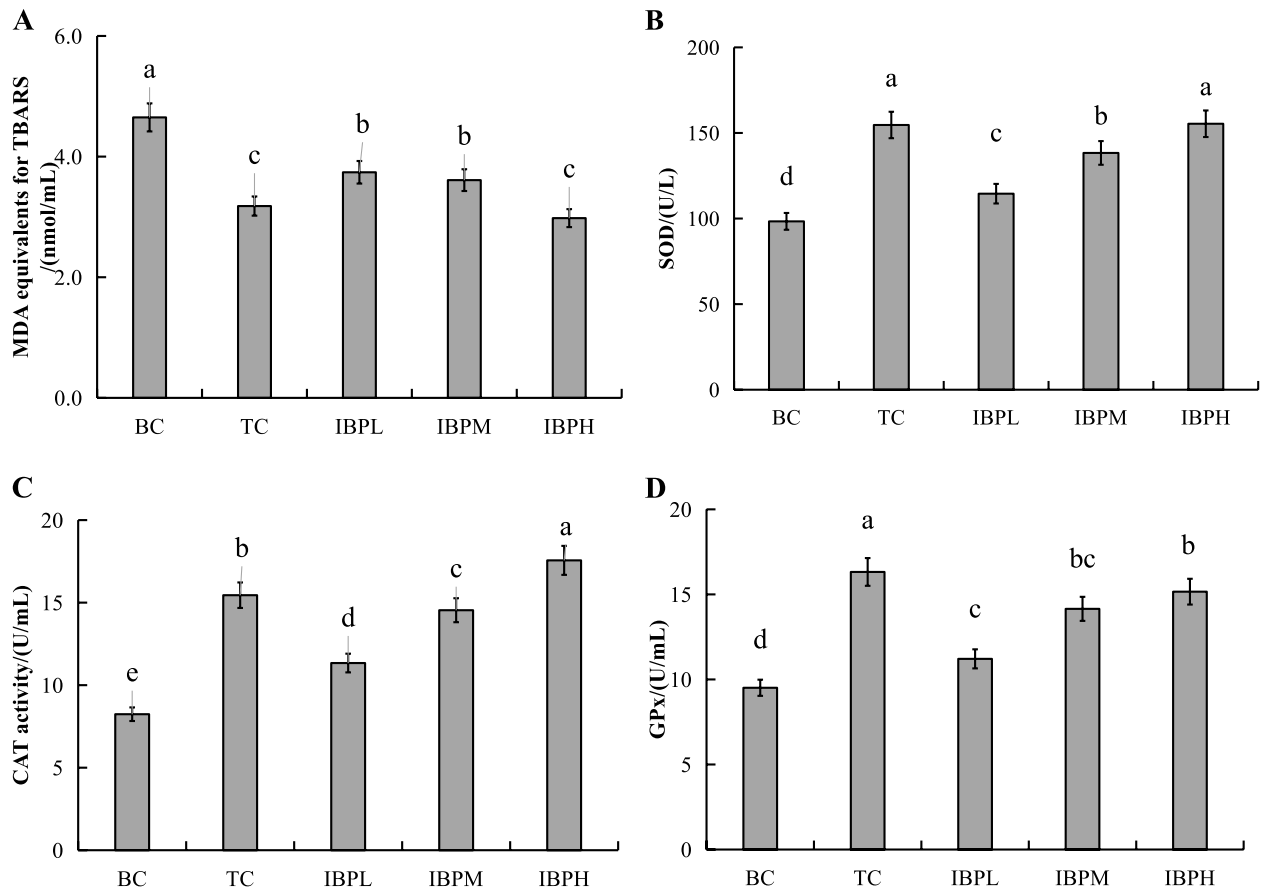


**Fig. 6** Effects of *Ipomoea batatas* polysaccharide (IBP) on liver antioxidant indices in exhaustive swimming mice (n=12). Note: Malondialdehyde (MDA), superoxide dismutase (SOD), catalase (CAT), and glutathione peroxidase (GPx)

GPx activities in the high-dose group were similar to those in the taurine control group. The above results indicated that IBP had strong antioxidant activity.

## Conclusions

IBP was identified, and its antifatigue activities were evaluated. No free monosaccharide was produced after simulated digestion of the IBP in vitro, but the structure of the polysaccharide changed, and the reducing sugar content increased. IBP could prolong the swimming time of exhausted mice and significantly improve their endurance. IBP could significantly improve the physical recovery ability of mice after excessive exercise and had a better effect on fatigue from exercise. This research revealed that the IBP effectively improved exercise endurance in mice and played a significant role in alleviating fatigue from exercise, providing new information for the development of nutritional supplements. However, this study describes the results of an antifatigue test based on animal tests; no human tests have been performed. Thus, there is still a certain distance from the development of antifatigue products, and further research is needed.

## Acknowledgements

The authors would like to thank the anonymous reviewers for their insightful comments and constructive suggestions.

## Authors' contributions

Conceptualization, X.G. and X.C.; methodology, X.G.; validation, X.G., W.M.; formal analysis, X.G.; resources, X.G., T.X.; data curation, X.G., L.L.; writing—original draft preparation, X.G.; writing—review and editing, X.C., L.L.; project administration, X.G.; funding acquisition, X.C.

## Funding

This research was funded by the Xinxiang Science and Technology project (GG2021022).

## Data availability

The datasets used and/or analyzed during the current study are available from the corresponding author upon reasonable request.

## Declarations

### Ethics approval and consent to participate

Not applicable.

### Consent for publication

Not applicable.

### Competing interests

The authors declare that they have no competing interests.

### Author details

<sup>1</sup>Xinxiang Institute of Engineering, Xinxiang 453700, China. <sup>2</sup>Xinxiang Institute, Xinxiang 453000, China.

Received: 10 June 2024 Accepted: 24 October 2024

Published online: 06 March 2025

## References

- An, Q., Li, G. Q., Li, X. T., Ju, R. J., & Shao, X. (2023). Extraction and refining process of polysaccharide from *tricholoma matsutake* and verification of its whitening effect. *Medical Plant*, *14*(1), 19–24.
- Bellenger, C. R., Fuller, J. T., Thomson, R. L., Davison, K., Robertson, E. Y., & Jonathan, D. (2016). Monitoring athletic training status through autonomic heart rate regulation: A systematic review and meta-analysis. *Sports Medicine*, *46*(7), 1461–1486.
- Chen, C. Y., Yuen, H. M., Lin, C. C., Hsu, C. C., Bernard, J. R., Chen, L. N., Liao, Y. H., & Tsai, S. C. (2021). Anti-false effects of santé premium silver perch essence on extreme swimming performance in rats. *Frontiers in Physiology*, *12*, e651972.
- Erika, H. A., & Pablo, M. (2018). Beneficial effects of naringenin in liver diseases: Molecular mechanisms. *World Journal of Gastroenterology*, *4*, 1679–1707.
- Gilstrap, S., Hobson, J., Owens, M., White, D., Sammy, M., Ballinger, S., & Goodin, B. (2021). Mitochondrial DNA copy number and damage in people with HIV and chronic pain. *The Journal of Pain*, *22*(5), 593.
- Huang, Y., Ge, R., Lou, G., Jiang, N., Zhu, X., Guo, Y., Liu, H., Liu, X., & Chen, X. (2023). The influence of dietary Coenzyme Q10 on growth performance, antioxidant capacity and resistance *Aeromonas hydrophila* of juvenile European eel (*Anguilla anguilla*). *Fish & Shellfish Immunology*, *138*, 108834.
- Huang, Y. X., Zhou, S. Y., Zhao, G. H., & Ye, F. Y. (2021). Destabilisation and stabilisation of anthocyanins in purple-fleshed sweet potatoes: A review. *Trends in Food Science and Technology*, *116*, 1141–1154.
- Iwuoha, V. O., & Abuajah, C. I. (2022). Sprouted sweet potato flour as a saccharification enhancer to import the brewing properties of pearl millet malt. *Journal of the Institute of Brewing*, *128*, 52–58.
- Lee, H. J., Jung, H., Cho, H., & Hwang, K. T. (2015). Anti-inflammatory effect of black raspberry seed oil in high-fat diet-induced obese mice. *Journal of Food Biochemistry*, *39*, 612–621.
- Lee, Y. K., Jung, S. K., & Chang, Y. H. (2020). Rheological properties of a neutral polysaccharide extracted from maca (*Lepidium meyenii* Walp.) Roots with prebiotic and anti-inflammatory activities. *International Journal of Biological Macromolecules*, *152*, 757–765.
- Li, B., Zhang, N., Feng, Q. S., Li, H., Wang, D., Ma, L., Liu, S., Chen, C. B., Wu, W., & Jiao, L. (2019). The core structure characterization and of ginseng neutral polysaccharide with the immune-enhancing activity. *International Journal of Biological Macromolecules*, *123*, 713–722.
- Liang, H. Y., Liu, Q., & Xiu, Y. H. (2021). Effects of marine drug propylene glycol alginate sodium sulfate on glucose and lipid metabolism in mice. *Material Plastic*, *58*, 150–154.
- Liu, W., Lad, M., & Foster, T. (2022). *In vitro* digestion of designed emulsions based on milk protein and guar gum systems. *Food & Function*, *13*, 6022–6035.
- Marzi, M., Rostami, C. M., & Zarenezhad, E. (2022). Hydrogels as promising therapeutic strategy for the treatment of skin cancer. *Journal of Molecular Structure*, *1262*, 133014.
- Mehta, R. K., & Agnew, M. J. (2012). Fluence of mental work on music endurance, false, and recovery during interim static work. *European Journal of Applied Physiology*, *112*, 2891–2902.
- Osman, W. N. W., & Mohamed, S. (2018). Standardized *Morinda Citrifolia* L. and *Morinda Elliptica* L. leaf extracts alleviated false by improving glycogen storage and lipid/carbohydrate metabolism. *Phytotherapy Research*, *32*, 2078–2085.
- Qu, Y., Ji, H., Song, W., Peng, S., Zhan, S. H., Wei, L. Y., Chen, M., Zhang, D., & Liu, S. C. (2022). The anti-false effect of the *Auxis thazard* oligopeptide via modulation of the AMPK/PGC-1  $\alpha$  path in me. *Food & Function*, *13*, 1641–1650.
- Shan, Y. Y., Jiang, B., Yu, J. H., Wang, J. Y., Wang, X. L., Li, H., Wang, C. M., Chen, J. G., & Sun, J. H. (2019). Protective effect of schisandra chinensis polysaccharides against the immunological liver injury in mice based on Nrf2/ARE and TLR4/NF- $\kappa$ B signaling pathway. *Journal of Medicinal Food*, *22*, 885–895.
- Tang, C., Sun, J., Zhou, B., Jin, C. H., Liu, J., Gou, Y. R., Chen, H., Kan, J., Qian, C. L., & Zhang, N. F. (2018). Immunomodulatory effects of polysaccharides from purple sweet potato on lipopolysaccharide treated RAW 264.7 macrophages. *Journal of Food Biochemistry*, *42*, e12535.
- Tian, C. Y., & Wang, G. L. (2008). Study on the anti-tumor effect of polysaccharides from sweet potato. *Journal of Biochemistry*, *136*, S351.

- Wei, W., Li, Z. P., Zhu, T., Fung, H. Y., Wong, T. L., Wen, X., Ma, D. L., Leung, C. H., & Han, Q. B. (2017). Anti-fatigue effects of the unique polysaccharide marker of *dendrobium officinale* on BALB/c mice. *Molecules*, *22*, 155.
- Yang, W. J., & Huang, G. L. (2021). Extraction, structural characterization, and physicochemical properties of polysaccharide from purple sweet potato. *Chemical Biology and Drug Design*, *12*, 3989–3993.
- Zhang, S., Liu, B., Yan, G., Wu, H., Han, H., & Cui, H. (2021). Chemical properties and anti-fatigue effect of polysaccharide from *Pholiota Nameko*. *Journal of Food Biochemistry*, *41*, 93–98.
- Zhang, X. M., Xie, L., Long, J. Y., Xie, Q. X., Zheng, Y., Liu, K., & Li, X. F. (2021). Salidside: A review of its recent advances in synthetic pathways and pharmaceutical properties. *Chemico - Biological Interactions*, *339*, 109268.
- Zhao, G., Kan, H., Li, J. Q., & Chen, Z. D. (2005). Characterization and immunostimulatory activity of an (1→6)- $\alpha$ -d-glucan from the root of *Ipomoea batatas*. *International Immunopharmacology*, *5*, 1436–1445.
- Zhao, H. P., Zhang, Y., Liu, Z., Chen, J. Y., Zhang, S. Y., Yang, X. D., & Zhou, H. L. (2017). Acute toxic and anti-fatigue activity of polysaccharide rich extract from cornsilk. *Biomedicine and Pharmacotherapy*, *90*, 686–693.
- Zhao, W. J., Zhang, W. Y., Liu, L., Cheng, Y. L., Guo, Y. H., Yao, W. R., & Qian, H. (2021). Fractionation, character and anti-fatigue activity of polysaccharides from *Brassica rapa. L* *Process Biochemistry*, *106*, 163–175.

### Publisher's Note

Springer Nature remains neutral with regard to jurisdictional claims in published maps and institutional affiliations.